Childhood leukemia: central nervous system abnormalities during and after treatment.

C Y Chen, R A Zimmerman, S Faro, L T Bilaniuk, T Y Chou and P T Molloy

AJNR Am J Neuroradiol 1996, 17 (2) 295-310
http://www.ajnr.org/content/17/2/295

Childhood Leukemia: Central Nervous System Abnormalities during and after Treatment

Cheng-Yu Chen, Robert A. Zimmerman, Scott Faro, Larissa T. Bilaniuk, Ting-Ywan Chou, and Patricia T. Molloy

PURPOSE: To document the radiologic abnormalities seen in the central nervous system (CNS) during and after treatment of childhood leukemia. **METHODS:** MR images (19 patients) and CT scans (12 patients) were reviewed retrospectively in 19 children and adolescents with neurologic complications of leukemia or its treatment. Patients were divided into two groups: the first included those with disease-related complications of leukemia, such as meningeal and parenchymal leukemia, chloroma, and cerebrovascular disorders; the second included patients with treatment-related neurotoxicity and infection caused by immunocompromised states. Pathologic confirmation of the CNS lesions was obtained in eight patients. Factors that predisposed to the development of tumor-related or treatment-related complications were determined by reviewing the medical records. **RESULTS:** Among the 19 patients, 10 had two or more different CNS abnormalities found on CT scans or MR images. The imaging abnormalities seen in 12 patients during treatment included sinus thrombosis (n = 3), transient gray or white matter ischemia (n = 2), presumed disseminated microinfarcts (n = 1), cerebral hemorrhage or infarct (n = 3), inflammatory demyelinating polyradiculoneuropathy (n = 1), infections (n = 4, 2 bacterial and 2 fungal), and meningeal leukemia (n = 2). After therapy, seven patients had CNS imaging abnormalities, including secondary brain tumors (2 malignant gliomas and 1 CNS lymphoma), spinal chloroma (n = 1), necrotizing leukoencephalopathy and mineralizing microangiopathy (n = 3), cerebral mucormycosis (n = 1), spontaneous intracranial hemorrhage (n = 3), and spinal meningeal leukemia (n = 1). **CONCLUSION:** The wide spectrum of CNS abnormalities that occur during and after treatment for leukemia is related to the inherent risk of the leukemia itself, to the treatment method, and to the duration of survival. Because many neurologic complications of leukemia are treatable, early diagnosis is essential.

Index terms: Leukemia; Children, diseases

AJNR Am J Neuroradiol 17:295–310, February 1996

Leukemia remains the most common form of childhood cancer, representing 3.7% of cancer deaths in the United States (1). In earlier years, central nervous system (CNS) complications of leukemia were rare because of the rapid fatality of the disease. More recently, with advances in treatment methods and consequent prolonged survival, the frequency of neurologic complications has increased (2, 3). CNS complications are caused either by the primary disease or by the therapy. Primary effects of the disease may include leukemic involvement of the leptomeninges, brain parenchyma, and cerebrovasculature (4). Treatment-related CNS complications may consist of white matter lesions, small-vessel calcifications, cerebrovascular disorders, secondary tumors, and infections (5–8). Both early and late CNS complications can be related to the neurotoxicity of the chemotherapeutic regimens (9, 10), radiation therapy (11), bone marrow transplantation (12), and immunosuppression caused by the disease itself or its treatment. Children and adolescents who survive the leukemia may contract endocrinopathy and/or

Received March 1, 1995; accepted after revision August 1.

From the Departments of Radiology (C-Y.C., R.A.Z., S.F., L.T.B.) and Neurology (P.T.M), The Children's Hospital of Philadelphia (Pa); and the Department of Radiology, Tri-Service General Hospital, National Defense Medical Center, Taipei, Taiwan, Republic of China (C-Y.C., T-Y.C.).

Address reprint requests to Robert A. Zimmerman, MD, Department of Radiology, The Children's Hospital of Philadelphia, 34th St & Civic Center Blvd, Philadelphia, PA 19104.

AJNR 17:295–310, Feb 1996 0195-6108/96/1702–0295

neurocognitive deficits caused by the late effects of the antileukemic treatment (13).

The clinical manifestations of CNS complications of leukemia that follow treatment are variable. Early recognition of these complications is important in order to institute treatment and increase the chances for overall survival. Several reports have described the usefulness of magnetic resonance (MR) imaging and computed tomography (CT) in the detection of those CNS complications (11, 14–17). We present the MR and CT features of CNS abnormalities in 19 children and adolescents with neurologic symptoms and signs that developed during or after antileukemic treatment. We discuss the potential relationship of the various CNS complications of the treatment methods, the duration of survival after initial treatment, and the timing of the clinical presentation.

Materials and Methods

Subjects

We retrospectively evaluated the cranial and spinal MR images and CT scans of 19 patients (14 male and five female) 8 months to 21 years old. The patients had various types of childhood leukemia, including 14 cases of acute lymphoblastic leukemia, 3 cases of acute myelogenous leukemia, 1 case of acute promyelogenous leukemia, and 1 case of mixed lineage leukemia (acute lymphoblastic leukemia and acute myelogenous leukemia). All initial MR images were obtained at the time of development of new neurologic symptoms and signs. Patients were examined during and after antileukemic treatment. Patients were divided into two groups: group 1 included 12 patients who had CNS abnormalities that occurred during therapy or within 3 months of completion of treatment; group 2 contained 7 patients with CNS abnormalities that occurred as late effects of leukemia.

The medical records were reviewed with attention to the type of treatment given, the time of onset of symptoms after the initial therapy and after the last therapy, and the outcome of the various CNS complications. The results of one postmortem neuropathologic examination and seven surgical biopsies of the brain and spinal lesions were reviewed. Neurologic development and psychosocial measurement were not evaluated.

Imaging Studies

In 18 of the 19 patients, MR images were obtained with two 1.5-T scanners (Siemens SP, Germany; Picker Vista HPQ, USA) during a period of 3 years (1991–1993). One patient, who was transferred for bone marrow transplantation, had MR imaging performed at another hospital. The 12 patients in group 1 were examined with MR or CT during or after the initiation of therapy. Among group 2 patients, imaging was performed at least 3 months after therapy was initiated. The imaging sequences consisted of spin-echo T1-weighted, 500–600/15–40/1–2 (repetition time/echo time/excitations), axial and sagittal images with 3- to 5-mm-thick sections obtained before and after intravenous injection of gadopentetate dimeglumine (0.1 mmol/kg) and T2-weighted, 2800–3000/90–120/1, axial and/or coronal images with 5-mm-thick sections. Additional coronal T1-weighted images were obtained when indicated. One patient with a spinal lesion was studied after intravenous injection of a triple dose of gadoteridol (0.3 mmol/kg). Two-dimensional time-of-flight MR angiography was performed in three patients in whom sinus thrombosis was evident on spin-echo MR images. The parameters used with this technique were as follows: 32/10/1; field of view, 20 to 22 cm; matrix, 192 × 256; flip angle, 50°; section thickness, 1.5 mm; section slab thickness, 3 to 7.5 cm. The scanning planes of the MR angiograms were axial, oblique-coronal, and sagittal, selected

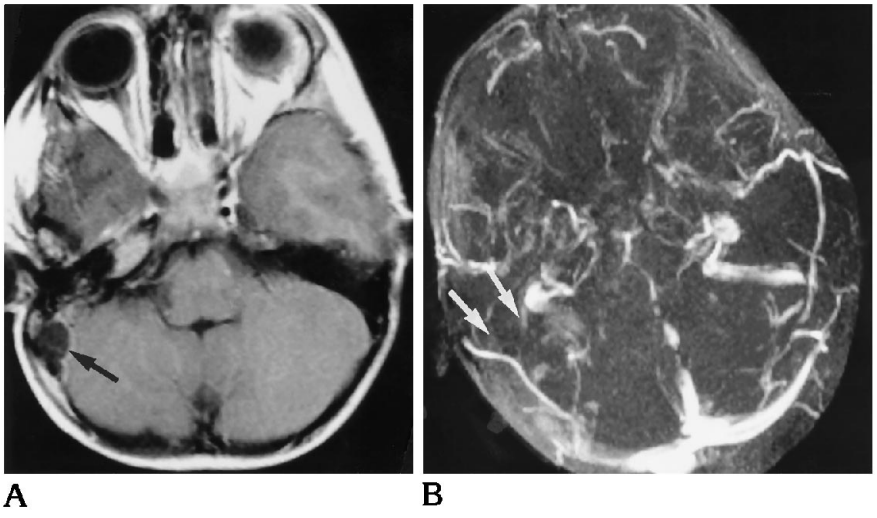

Fig 1. Case 1: 5-year-old girl with sinus thrombosis, which occurred during the first course of chemotherapy for acute promyelogenous leukemia.

A, Contrast-enhanced T1-weighted image shows hypointense filling defect in the right sigmoid sinus (*arrow*).

B, MR angiogram (32/10,50° flip angle) shows no flow in the right sigmoid sinus and jugular vein (*arrows*).

for different segments of the dural sinuses. Ten patients had two or more follow-up MR studies. Twelve patients also had CT studies and four of these had serial cranial CT scans before CNS complications developed.

Results

Among the 19 patients who had received antileukemic treatment, 12 had early CNS complications identified on MR images and CT scans. These included sinus thrombosis (n = 3) (Fig 1), transient gray or white matter ischemia (n = 2) (Figs 2 and 3), presumed disseminated microinfarcts (n = 1) (Fig 4), cerebral hemorrhage or infarct (n = 3), inflammatory demyelinating polyradiculoneuropathy (n = 1) (Fig 5), infection (2 bacterial [Figs 6 and 7] and 2 presumed fungal [Figs 8 and 9]), and cerebrospinal meningeal leukemia (n = 2). The second group, with CNS complications that occurred late, comprised seven patients with the following lesions: three secondary brain tumors, including glioblastoma multiforme (Fig 10), anaplastic astrocytoma (Fig 11), and B-cell lymphoma (Fig 12); one spinal epidural chloroma (Fig 13); three necrotizing leukoencephalopathies and mineralizing microangiopathy (Fig 14); one isolated cerebral mucormycosis (Fig 15); three intracranial hemorrhages; and one spinal meningeal leukemia.

In group 1, four cerebrovascular events were believed to be related to asparginase therapy and included two sinus thromboses, one spontaneous hemorrhage, and one case of reversible cortical ischemia. Two patients were thought to have disseminated microabscesses of the brain caused by fungal infections. No fungus was found on cultures from urine, blood, and cerebrospinal fluid (CSF). Even the brain specimen from open biopsy in case 12 failed to show the causative organism. Both patients improved clinically and radiologically after empiric treatment with amphotericin. In group 2, irreversible necrotizing leukoencephalopathy and calcification of basal ganglia and subcortical white matter were identified in three patients with acute lymphoblastic leukemia who were treated with combined irradiation and intrathecal methotrexate 5 to 7 years earlier. The brain calcification in case 14 was seen as early as 3 years after treatment. The clinical profiles of the 19 patients are given in the Table.

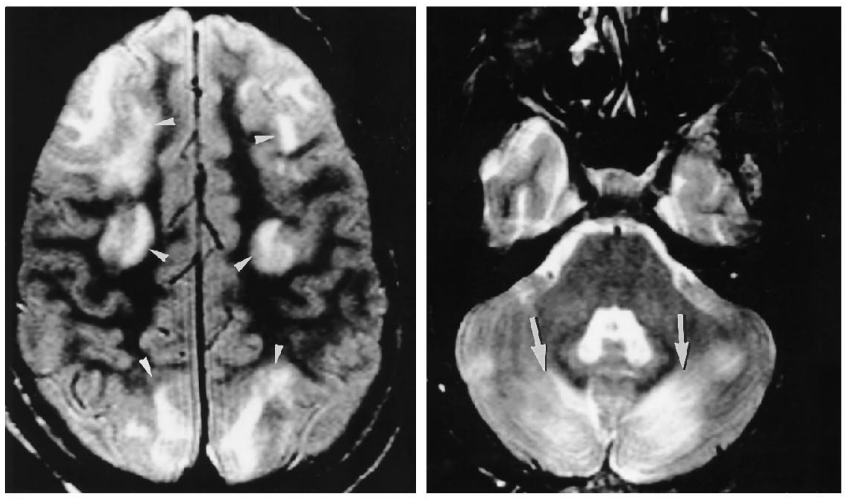

Fig 2. Case 2: 16-year-old boy with cerebral and cerebellar cortical ischemia, which occurred during chemotherapy for acute lymphoblastic leukemia.

A and *B*, MR images show symmetrical high-signal lesions in the bilateral frontoparietal and parietooccipital lobes (*arrowheads*) on proton density–weighted image (*A*) and in cerebellar cortices (*arrows*) on T2-weighted image (*B*). A follow-up MR study 6 months later showed complete resolution of the ischemic cortical lesions (*not shown*).

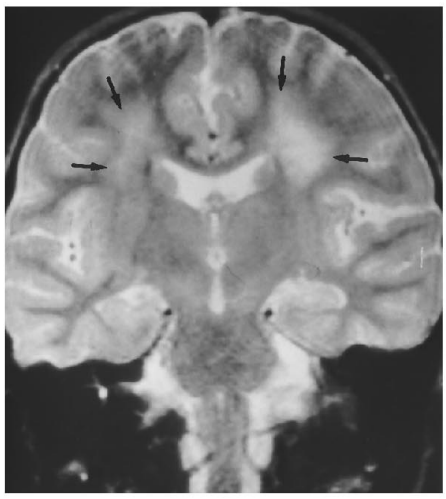

Fig 3. Case 3: 5-year-old boy with bilateral cerebral white matter edema or demyelination, which occurred 3 weeks after last intravenous injection of methotrexate to treat acute lymphoblastic leukemia. Coronal T2-weighted MR image shows high-signal lesions in the bilateral periventricular white matter and centrum semiovale (*arrows*). The white matter lesions disappeared completely on a follow-up MR image 2 months later when patient was symptom-free.

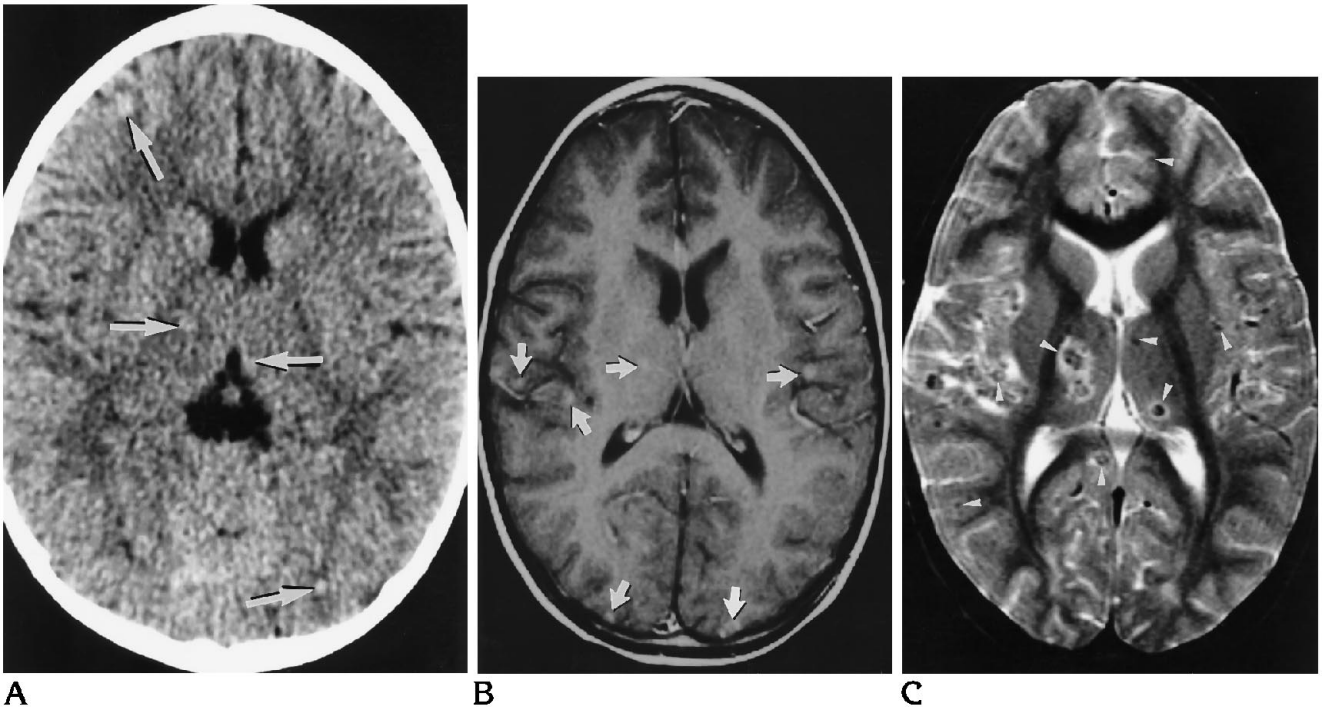

Fig 4. Case 4: 3-year-old boy with presumed disseminated microinfarcts, which occurred during treatment for acute myelogenous leukemia.

A, Noncontrast CT scan shows multiple small hyperdensities in the superficial brain and thalami (*arrows*).

B, The small cerebral lesions were slightly hyperintense (*arrows*) on postcontrast T1-weighted MR image.

C, Corresponding T2-weighted image shows more lesions (*arrowheads*) with hypointense signal intensity in the superficial brain. Lesions in the thalami also had perifocal edema. These small lesions resolved completely on follow-up MR images (*not shown*).

The MR and CT findings of the CNS abnormalities in the 19 patients with leukemia are similar to the neuroimaging characteristics seen in patients with the same CNS abnormalities (ie, hemorrhages, infarcts, meningitis, sinus thrombosis, and malignant glioma) but without leukemia. The MR findings in patient 16, who had CNS B-cell lymphoma after bone marrow transplantation, and in patient 1, who had presumed disseminated microinfarcts, have not previously been reported. The CNS B-cell lymphoma appeared hyperintense on plain CT scans and hypointense on T1- and T2-weighted MR images (Fig 12). The tumor did not enhance after intravenous contrast administration on either CT scans or MR images. The patient with disseminated microinfarcts had multiple tiny areas of low signals with mild perifocal edema in the cerebrum and brain stem on T2-weighted MR images. The microinfarcts were slightly hyperintense on T1-weighted images (Fig 4).

Discussion

Owing to advancements in antileukemic treatment, by 1990, one in every 2000 young people who reached the age of 20 was a survivor of childhood acute lymphoblastic leukemia (18). With improved survival, the neurologic complications of antileukemic treatment have also increased. Currently, many of the CNS complications seen in connection with acute lymphoblastic leukemia are related to the neurotoxicities of various chemotherapeutic regimens, such as methotrexate (19), cytaribine (20), the acute and delayed effects of CNS radiation (21), the adverse effects of bone marrow transplantation (22), coagulopathy caused by the disease or by asparaginase (10), and breakdown of the immune mechanism resulting from the leukemia itself or from bone marrow suppression with intense chemotherapy.

The CNS complications that occurred early in the leukemic course were frequently cerebro-

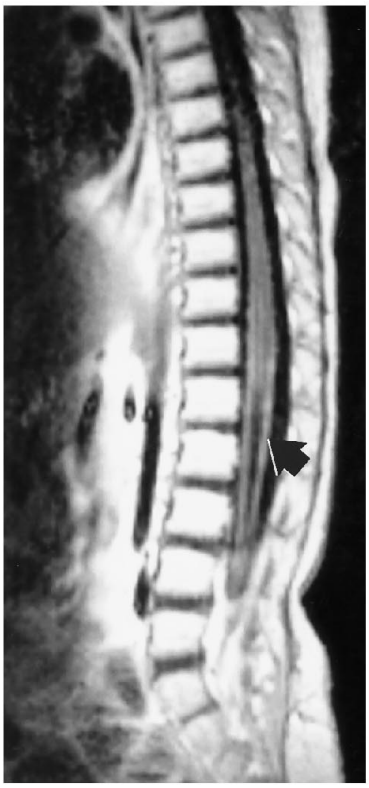

Fig 5. Case 8: 8-month-old infant with inflammatory demyelinating polyradiculoneuropathy had limb weakness and urinary retention during treatment for mixed lineage leukemia. Sagittal T1-weighted MR image of the spine after injection of a triple dose of gadoteridol (3 mmol/kg) shows enhancement of the lumbosacral roots (*arrow*).

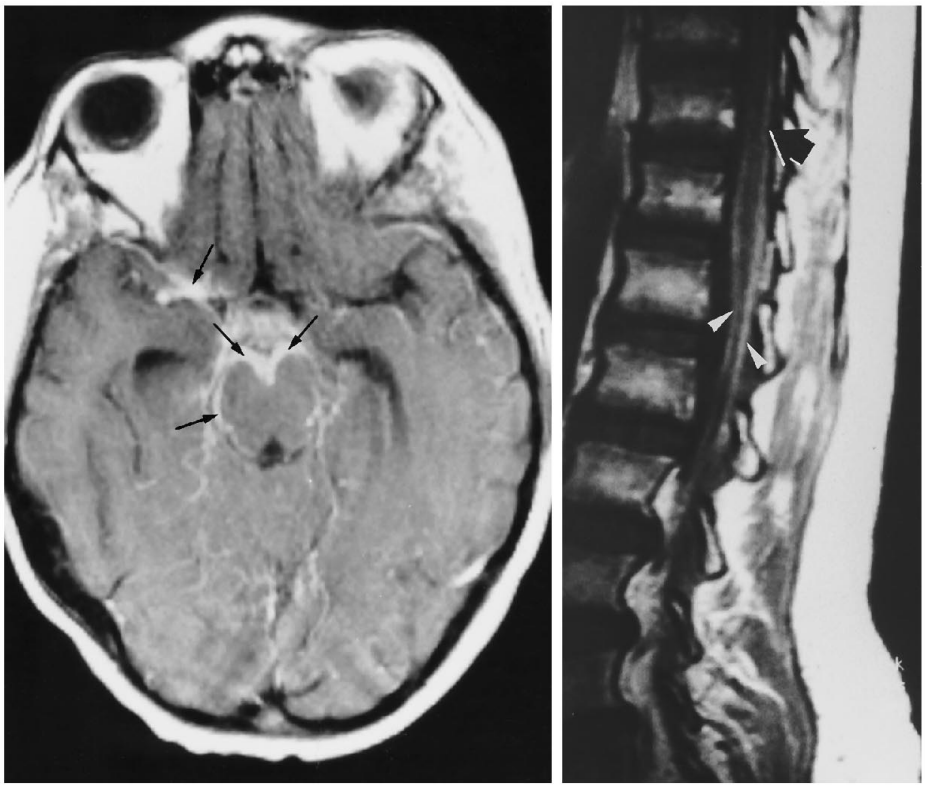

A B

Fig 6. Case 9: 12-year-old boy with purulent meningitis, which occurred at the end of repeat chemotherapy to treat acute lymphoblastic leukemia.

A, Postcontrast T1-weighted MR image of the brain shows enhancing exudate in the basal cisterns (*arrows*).

B, Sagittal contrast-enhanced T1-weighted MR image of the spine shows enhancement of the leptomeninges of the spinal cord and roots (*arrow* and *arrowheads*).

vascular disorders and infections. Of nine patients with cerebrovascular accidents, four were related to asparginase. Two patients with superior sagittal sinus thrombosis treated with asparginase (cases 5 and 6) improved clinically, presumably as a result of fresh frozen plasma therapy. Follow-up MR imaging (case 5) showed partial resolution of the thrombus in the superior sagittal sinus. One patient (case 6) had venous infarct complicating the dural sinus thrombosis. Another patient (case 2) with transient cortical ischemia after intravenous administration of asparginase completely recovered after treatment was discontinued: a follow-up MR image showed total resolution of the ischemic cortical lesions. Treatment with asparginase leads to the depletion of plasma proteins involved in both coagulation and fibrinolysis and has been linked to cerebrovascular complications, including cortical infarct, intracerebral hemorrhage, hemorrhagic infarct, and dural sinus thrombosis (10, 23, 24).

Cerebrovascular thrombosis or hemorrhage can also occur in the course of antileukemic treatment as a result of leukocytosis, thrombocytopenia, sepsis, and coagulopathy (25, 26, 27). One patient with acute myelogenous leukemia (case 4) presented with encephalopathy and had CT and MR imaging findings that were consistent with disseminated microinfarcts, which were thought to be related to leukocytosis. Multiple microinfarcts associated with small-vessel thromboses have previously been observed in patients with malignant tumors in whom a syndrome of global encephalopathy developed (28). The presumed multiple small-

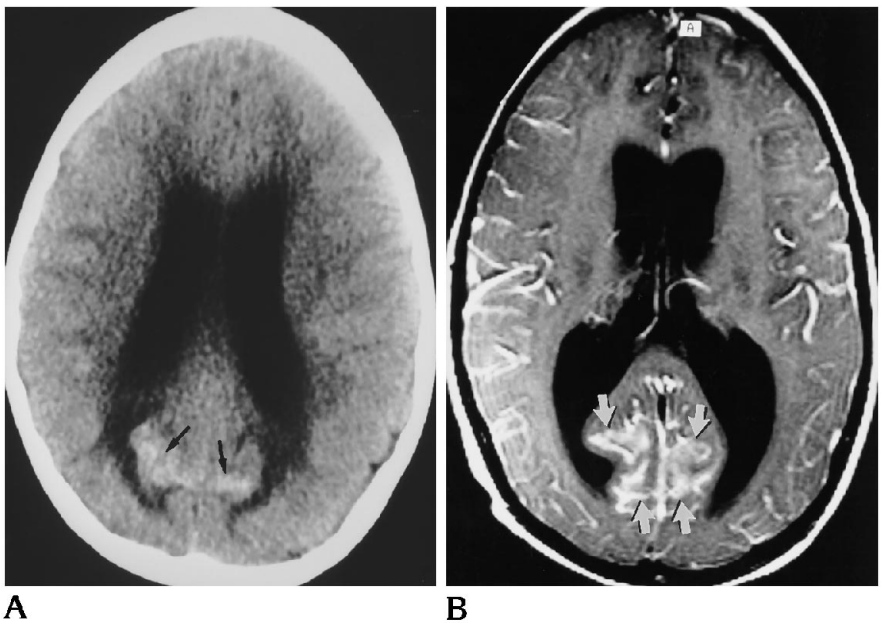

Fig 7. Case 10: 9-year-old girl with acute lymphoblastic leukemia had hemorrhagic infarcts of bilateral occipital lobes and superimposition of leptomeningeal leukemia and meningitis related to *Acinetobacter* infection.

A, Noncontrast CT scan shows hemorrhage of the occipital lobes (*arrows*) along with dilatation of the lateral ventricles caused by communicating hydrocephalus.

B, Postcontrast T1-weighted MR image at the level of the lateral ventricle shows diffuse enhancement of the brain surface. The high signal enhancement was even more conspicuous in the hemorrhagic area of the occipital lobes (*arrows*).

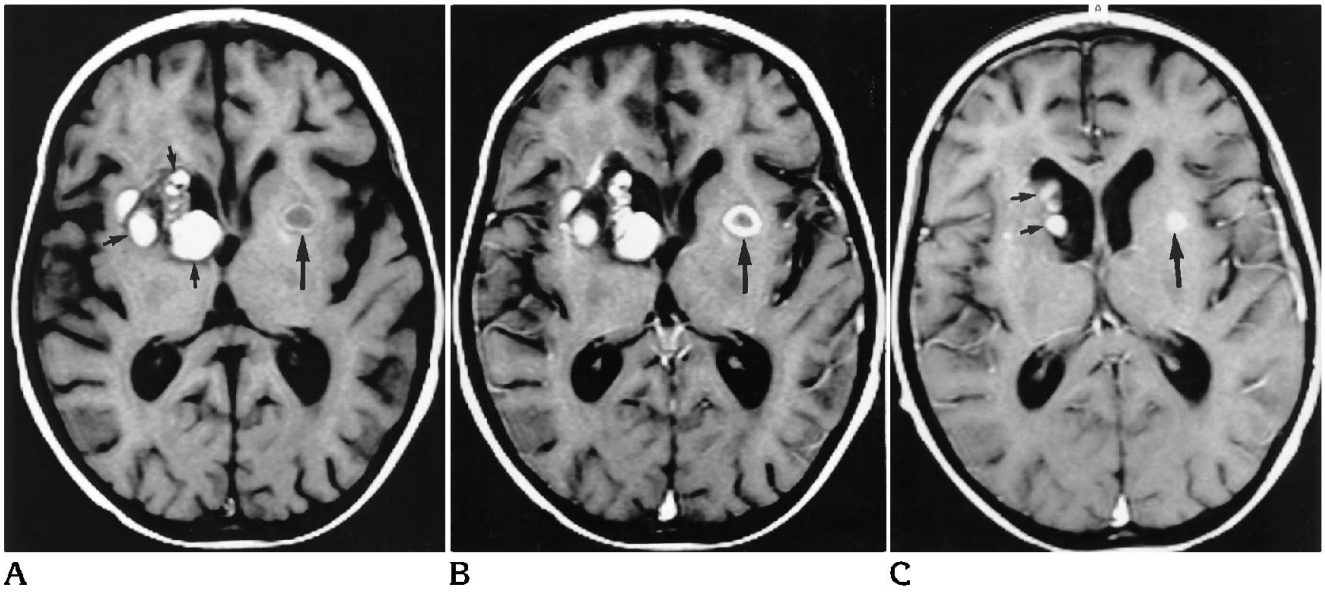

Fig 8. Case 11: 11-year-old girl with presumed systemic and cerebral candidiasis, which developed during repeat chemotherapy for acute lymphoblastic leukemia.

A, T1-weighted MR image shows a rimlike lesion (*large arrow*) with hyperdense wall and internal hypodensity in the left putamen. The lesion with complex high and low signals (*small arrows*) in the right basal ganglia was caused by previous spontaneous hemorrhage.

B, Postcontrast T1-weighted MR image shows rimlike enhancement of the left putaminal lesion (*arrow*). More enhancing small nodules were found in the right superior frontal region, the left parietal lobe, and the inferior frontal regions (*not shown*).

C, A follow-up contrast-enhanced T1-weighted MR image obtained after empiric treatment with amphotericin B shows a decrease in the size of the lesion in the left putamen (*large arrow*) and of the hematoma in the right basal ganglia (*small arrows*).

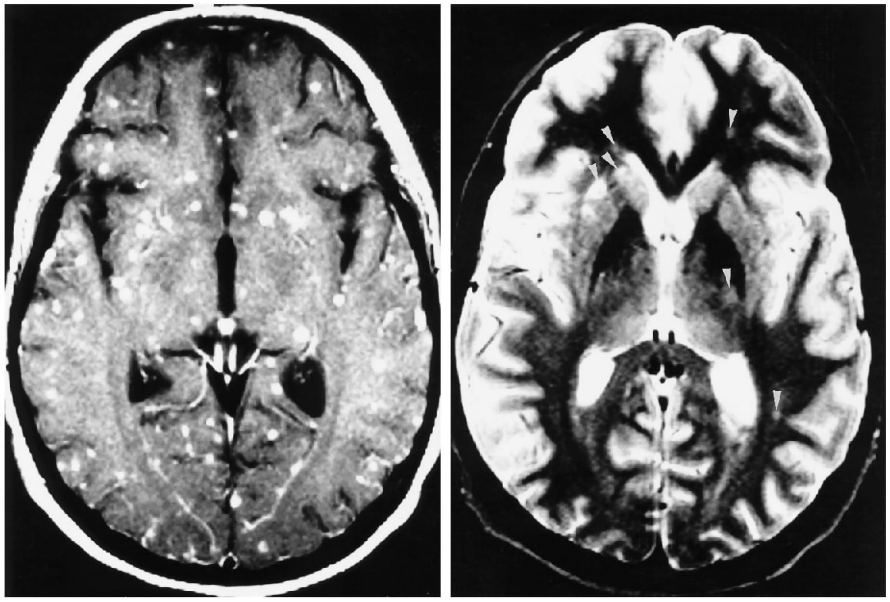

Fig 9. Case 12: 13-year-old boy with fever and headache associated with presumed fungal infection, which occurred during treatment for acute myelogenous leukemia.

A, Postcontrast T1-weighted MR image shows disseminated enhancing nodules in the brain parenchyma.

B, The signal of the nodules was inconspicuous on this T2-weighted MR image (*arrowheads*).

vessel thromboses in this patient appeared as multiple tiny areas of low signal intensity in the brain parenchyma and brain stem on T2-weighted images and as areas of mild hyperintense signal intensity on T1-weighted images without contrast enhancement. An unenhanced CT scan obtained at the same time showed few tiny hyperintense lesions in the brain. On the basis of the imaging characteristics, the tiny lesions appeared to be small intravascular thrombi, and they resolved completely after conservative treatment.

During chemotherapy with all-trans retinoic acid, one patient with acute promyelogenous leukemia (case 1) had acute onset of seizure and left-sided limb weakness, resulting from thrombosis of the right sigmoid sinus (Fig 1) and leukostasis. Acute promyelogenous leukemia itself is a disease in which disseminated intravascular coagulopathy is to be expected (26). In a study by Kantarjian et al (29), as many as 26% of patients with acute promyelogenous leukemia had early fatal hemorrhage associated with disseminated intravascular co-

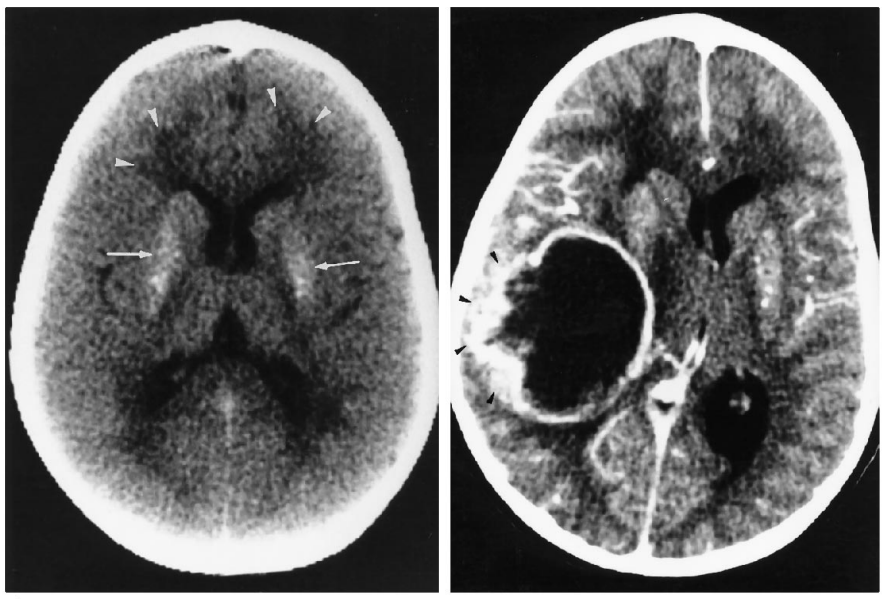

Fig 10. Case 14: 9-year-old boy with secondary glioblastoma multiforme, which developed 5 years after last chemotherapy for acute lymphoblastic leukemia.

A, Noncontrast CT scan obtained 3 years after initial combined treatment with irradiation and intrathecal chemotherapy shows calcifications (*arrowheads*) in the subcortical regions of the right superior frontal lobe. Basal ganglia are also calcified (*arrows*).

B, Postcontrast CT scan obtained 2 years after that in *A* shows a big rimlike enhancing mass with irregularity of the lateral wall (*arrowheads*).

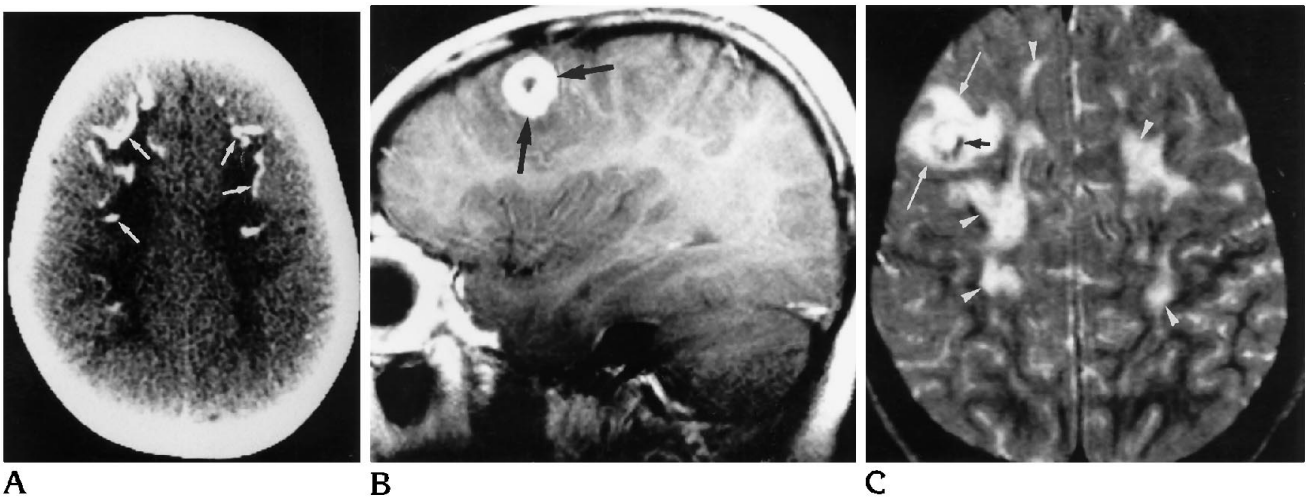

Fig 11. Case 15: 12-year-old boy with anaplastic astrocytoma, which developed 5.5 years after therapy for acute lymphoblastic leukemia.

A, Noncontrast CT scan obtained 3 years after initial combined treatment with irradiation and intrathecal chemotherapy shows calcifications (*arrows*) in the subcortical region of the frontoparietal lobes.

B, Postcontrast parasagittal T1-weighted MR image obtained 3 years after that in *A* shows an enhancing mass (*arrows*) in the right superior frontal lobe.

C, The right superior frontal mass appeared as a lesion of high signal intensity (*white arrows*) with a central rim of hypointensity (*black arrow*) on axial T2-weighted MR image. Symmetrical high signals (*arrowheads*) in the high convexity of the parietal white matter were caused by delayed radiation injury.

Fig 12. Case 16: 11-year-old boy with multiple B-cell lymphomas, which occurred 4 months after bone marrow transplantation for treatment of acute lymphoblastic leukemia.

A, Postcontrast T1-weighted MR image at the level of the foramen of Monro shows unenhancing masses in the left basal ganglia and left frontal lobe (*arrows*) and in the right cerebellar hemisphere (*not shown*).

B, On T2-weighted image, the masses are hypointense (*arrows*) relative to the cerebral cortex, with mass effect and considerable high-signal vasogenic edema.

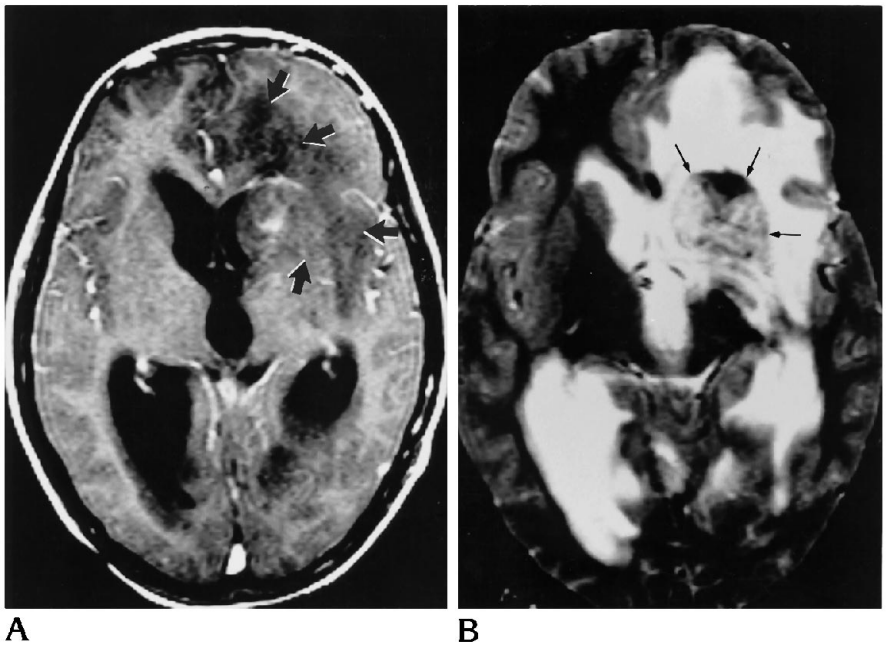

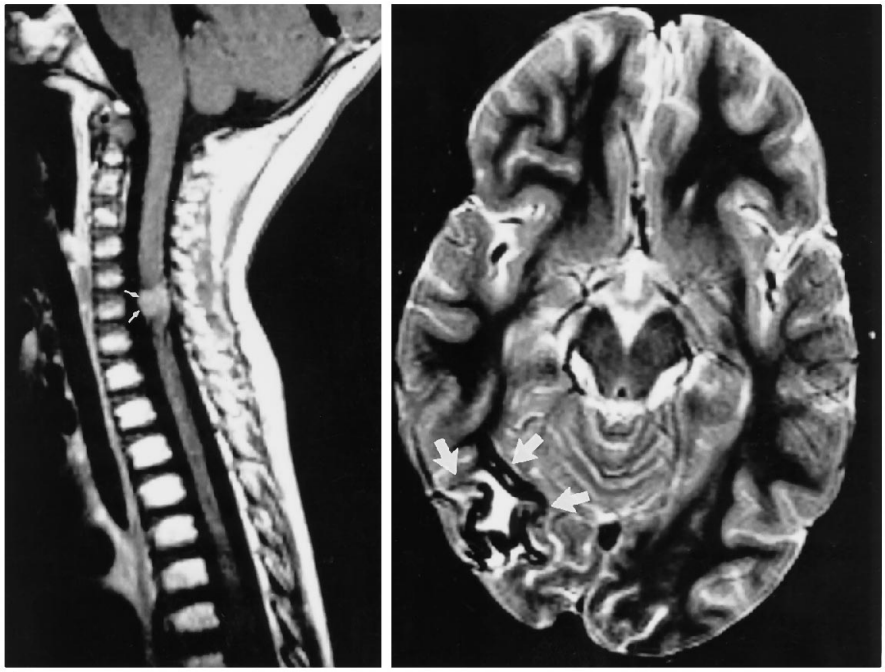

Fig 13. Case 17: 3-year-old boy with spinal epidural chloroma and cerebral hemorrhagic infarct, which developed 1 year after treatment for acute myelogenous leukemia.

A, Sagittal postcontrast T1-weighted image shows the enhancing epidural mass (*arrows*) within the spinal canal.

B, Axial T2-weighted MR image of the brain shows subacute hemorrhagic infarct with gyriform low signals (*arrows*) in the right occipital lobe.

Fig 14. Case 19: 7-year-old boy with mineralizing arteriopathy, which developed after 5 years of combined therapy with irradiation and intradural methotrexate for treatment of acute lymphoblastic leukemia. Postcontrast T1-weighted MR image shows high-signal lesions (*arrows*) in the bilateral basal ganglia, thalami, and frontal and occipital subcortical regions. The high-signal lesions were present on noncontrast T1-weighted images (*not shown*).

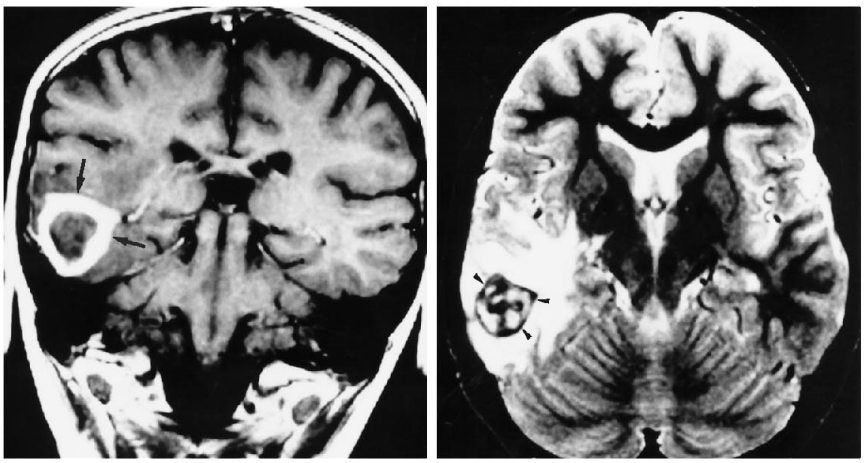

Fig 15. Case 13: 7-year-old boy with cerebral mucormycosis, which occurred 3 months after treatment for acute lymphoblastic leukemia.

A, Coronal postcontrast T1-weighted MR image shows rim-enhancing mass (*arrows*) in the right posterior temporal lobe.

B, On T2-weighted MR image, the mass appears hypointense (*arrowheads*) relative to the cerebral cortex, with considerable high-signal vasogenic edema.

Nineteen patients with CNS abnormalities during and after antileukemic treatment

Case*	Age, y/ Sex	Leukemia Type	Treatments†	Interval A/I‡	Symptoms and Signs	CNS Abnormalities	Autopsy, Biopsy, or CSF Study	Outcome	MR Findings	CT Findings
1	5/F	APML	RA	5/during first course of chemo	Seizure, L limb weakness	Sinus thrombosis, R sigmoid sinus	Partial autopsy	Died	Enhanced thombus in R sigmoid sinus on T1 with Gd; MRA showed no flow in R sigmoid sinus	High-density blood clot in R sigmoid sinus
2	16/M	ALL	Asp, VCR, adr, dexa	16/2 d after asp	Seizure	Multiple cortical ischemia	NP	Recovered	Increased signal of bilateral parietal and cerebellar cortices on T2	NP
3	5/M	ALL	IV MTX, VCR, asp	5/3 wk after last IV MTX	Change of mental status	Bilateral WM edema or demyelination	NP	Recovered	Symmetrical HS in bilateral periventricular WM on T2	NP
4	3/M	AML	IT MTX, ara-C, dauno	3/during first course of chemo	Encepha-lopathy	Presumed disseminated microinfarcts	NP	Improved	Disseminated tiny LS in brain on T2 and T2*; on T1 they were fewer and mildly hyperintense	Scattered tiny high densities in thalami and cerebral white matter
5	9/F	ALL	IT MTX, salvage, ara-C, asp	2/1 mo after salvage chemo	Seizure, fever	R occipital infarct	NP	Improved	Focal high signal in R occipital cortex on T2	Subtle low density in R occipital cortex
6	15/M	ALL	IV MTX, VCR, asp	15/4th wk during first course	Seizure, L hemiparesis	SSS thrombosis	NP	Improved	Enhanced thrombus in SSS on T1 with Gd; MRA showed no flow in SSS	NP
7	12/M	ALL	RT, IT MTX, asp, VCR	11.6/5 d after last asp	L hemiparesis	SSS thrombosis with venous infarct of R occipital lobe	NP	Improved	Poor visualization of SSS and R transverse sinus on T1 with Gd and MRA; HS in R occipital lobe on T2	NP
8	0.6/F	Mixed-lineage leukemia	IT and IV ara-C, asp, VCR	0.6/3rd wk during first course of chemo	Limbs weakness, urinary retention	Inflammatory demyelinating polyradiculo-neuropathy	1. Biopsy 2. Negative CSF culture and cytology	Improved	Enhancement of cauda equina on T1 with Gd	NP
9	12/M	ALL	IT MTX, asp, VCR, dauno	10.5/at the end of second course	Change of mental status	1. Purulent meningitis 2. Multiple infarcts	Autopsy	Died	Enhancement of basal cisterns and leptomeninges of brain and spinal cord on T1 with Gd	Multiple low densities in bilateral basal ganglia and right temporoparietal and occipital lobe

10	9/F	ALL	RT, IV and IT MTX, asp, VCR, dauno	7.5/6 d	Seizure	1. Occipital hemorrhagic infarct 2. Meningitis 3. Meningeal leukemia	1. Positive CSF culture for *Acinetobacter* 2. Positive CSF cytology for leukemia	Died	Leptomeningeal enhancement on T1 with Gd; gyriform low signals in bilateral occipital lobe on T2; ventricular dilatation	Gyriform high densities in bilateral occipital lobe; ventricular dilatation
11	11/F	ALL	Asp, VCR, ara-C	6.5/during second course	Change of mental status, fever	1. Cerebral hemorrhage 2. Presumed candidiasis	CSF and urine culture negative	Improved	Scattered hyperintense rimlike nodules in brain on T1 that were enhanced on T1 with Gd and mixed hyper- and hypointensity on T2	Multiple enhancing nodules in brain; hematoma in R basal ganglia; disseminated tiny hypodensities in liver, spleen, and kidneys
12	13/M	AML	Dauno, ara-C, VP-16, 6-TG	12.5/during second course of chemo	Fever, headache, vasomotor instability	1. Vasculopathy 2. Presumed fungal infection	1. Biopsy 2. CSF culture negative	Improved	Disseminated enhancing nodules in brain on T1 with Gd; the signal of nodules was inconspicuous on T1 and T2	NP
13	7/M	ALL	RT, IT MTX, CHP540	4/3 mo	. . .	Mucormycoma, R temporal lobe	Biopsy	Died	R temporal lobe mass hypointense on T1, rim enhancement on T1 with Gd and hypointense on T2	. . .
14	9/M	ALL	RT, IT MTX, VCR, asp, pred, BMT	2/5 y	Acute loss of vision, L limb weakness, headache, vomiting	1. MA 2. DL 3. GBM, R temporoparietal lobe	Biopsy	Died	Irregular rim-enhancing mass in R temporoparietal lobe on T1 with Gd; HS in periventricular WM on T2	Calcification of bilateral basal ganglia; irregular rim-enhancing mass in R temporoparietal lobe
15	12/M	ALL	RT, IT MTX, IT and IV ara-C, asp	6.5/5.5 y	Seizure	1. MA 2. DL 3. Anaplastic astrocytoma, R frontal lobe	Biopsy	Died	Rim-enhancing mass in R frontal lobe on T1 with Gd; HS in periventricular WM on T2	Symmetrical subcortical calcification of bilateral frontal and occipital lobes
16	11/M	ALL	RT, IT and IV MTX, BMT, asp, VCR	6.5/4 mo after last BMT	Acute mental status change	Multiple B-cell lymphomas in R cerebellum and L basal ganglia and L frontal lobe	Biopsy	Died	Unenhancing hypointense masses in R cerebellar hemisphere, L basal ganglia, and L frontal lobe on T1 with Gd and T2	Unenhancing hyperintense masses in R cerebellar hemisphere, L basal ganglia, and L frontal lobe
17	3/M	AML	RT, IT MTX, BMT, high-dose IV ara-C	1/1 y	Stroke, thrombocytopenia	1. Hemorrhagic infarct, R occipital lobe 2. Epidural chloroma at C-6	Biopsy	. . .	Enhancing epidural mass at C-6 level on T1 with Gd; gyriform low signals in R occipital lobe on T2	Gyriform high density in R occipital lobe

TABLE—continued

Case*	Age, /y Sex	Leukemia Type	Treatments†	Interval A/I‡	Symptoms and Signs	CNS Abnormalities	Autopsy, Biopsy, or CSF Study	Outcome	MR Findings	CT Findings
18	21/M	ALL	RT, IT MTX, BMT	16/5 mo after BMT	Headache, thrombocytopenia	1. Spinal leptomeningeal leukemia 2. Cerebral hemorrhage	CSF cytology positive for leukemia	Died	Enhancement of cauda equina on T1 with Gd	Several cerebral and tentorial hematomas
19	7/M	ALL	RT, IT MTX, 6-MP, decadron	2/1 y after last therapy	Headache, change of mental status	1. MA 2. DL 3. Subdural hematoma	NP	Deteriorated	HS in bilateral basal ganglia and subcortical WM on T1 and HS in periventricular WM on T2; R occipital subdural LS on T1	Calcification of bilateral basal ganglia and subcortical WM, R frontotemporal subdural fluid collection

* Cases 1 to 12 are in group 1; cases 13 to 19 in group 2.

† Most treatment methods and drugs that were used in the last course of chemotherapy are listed.

‡ A indicates the age (years) when the diagnosis of leukemia was made. I indicates the interval between the last antileukemic treatment and the onset of neurologic symptoms.

Note—Adr = adriamycin; ALL = acute lymphoblastic leukemia; AML = acute myelogenous leukemia; APML = acute promyelogenous leukemia; ara-C = cytarabine; asp = asparginase; BMT = bone marrow transplantation; chemo = chemotherapy; CHP540 = Children's Hospital of Philadelphia protocol 540; dauno = daunomycin; dexa = dexamethasone; DL = diffuse necrotizing leukoencephalopathy; GBM = glioblastoma multiforme; Gd = gadopentetate dimeglumine; HS = high signals; IT = intrathecal; IV = intravenous; LS = low signals; MA = mineralizing arteriopathy; MRA = magnetic resonance angiography; MTX = methotrexate; NP = not performed; pred = prednisolone; RA = retinoic acid; RT = radiation therapy; SSS = superior sagittal sinus; T1 = T1-weighted images; T2 = T2-weighted images; T2* = T2* gradient-echo images; VCR = vincristine; VP-16 = etoposide; WM = white matter; 6-MP = 6-mercaptopurine; 6-TG = 6-thioguanine.

agulopathy that occurred during the first course of therapy. More recently, the use of all-trans retinoic acid to achieve remission in acute promyelogenous leukemia has reduced the rate of occurrence of coagulopathy in these patients (30).

One patient (case 3) had a reversible encephalopathy after intravenous methotrexate treatment for acute lymphoblastic leukemia (Fig 3). Clinical symptoms improved and follow-up MR imaging showed complete absence of the high-signal-intensity white matter abnormalities seen previously on T2-weighted images. A reversible encephalopathy in patients with acute lymphoblastic leukemia may occur with the use of intravenous methotrexate or high-dose cytaribine. White matter appears hypodense on CT scans (31) with corresponding high signal on T2-weighted MR images (19, 20). The histopathology of the white matter lesions remains unknown, although white matter edema or demyelination has been suggested (14, 20).

Bacterial or fungal infections associated with neutropenia are common in patients with newly diagnosed or recurrent acute leukemia (32, 33). Three of our five patients with CNS infections had persistent neutropenia. One patient (case 9) with purulent meningitis had enhancement of the leptomeninges of the basal surface of the brain and spinal cord on postcontrast T1-weighted MR images (Fig 6). A follow-up CT scan before death showed multiple infarcts resulting from infection-induced vasculitis, a finding verified at autopsy. Among the three patients with fungal infections, one (case 13) had pathologically proved cerebral mucormycosis. Isolated cerebral mucormycosis is uncommon and usually results from extension of preexisting infection by a species of *Mucor* in the nose or paranasal sinuses (rhinocerebral mucormycosis) (34, 35). A preoperative imaging diagnosis of cerebral mucormycosis is difficult. The hypointense signal intensity of the mucormycosis seen on T2-weighted images (Fig 15B) is not understood, although a recent study suggested that the low signal intensity of *Aspergillus fumigatus* on T2-weighted and gradient-echo MR images was caused by accrual of the paramagnetic substances, such as iron, manganese, magnesium, and zinc (36). Microbiological documentation of CNS fungal infection (cases 11 and 12) was not obtained, despite cultures from urine, blood, and CSF. In case 11, both CT and MR imaging revealed rimlike enhancing nodules in the brain (Fig 8), whereas abdominal CT scans showed disseminated unenhancing hypodense nodules in the liver, spleen, and kidneys, consistent with CNS and systemic candidiasis. The patient showed both clinical and radiologic improvement after empiric antifungal treatment with amphotericin. In case 12, the MR imaging findings of disseminated enhancing nodules in the brain and cerebellum (Fig 9) prompted open biopsy of the cerebral lesions. Microscopic examination together with several special stains of the brain specimens revealed abnormal thickening of the vessel wall and scattered infiltration of inflammatory cells but no fungus or bacteria. The patient was treated empirically for fungus, and the symptoms disappeared. Follow-up MR imaging showed complete resolution of the cerebral lesions. In some cases, MR imaging may be more sensitive than routine cultures in demonstrating anatomic evidence of clinically suspected CNS fungal infection and in monitoring the response to treatment.

CNS arachnoiditis may occur with intrathecal administration of chemotherapeutic agents such as methotrexate or cytaribine. Other causes of nerve root enhancement on contrast-enhanced MR images of patients with leukemia include postsurgical or postcontrast arachnoiditis (37), mechanical root compression with associated inflammation (37), cytomegalovirus polyradiculopathy in patients with acquired immunodeficiency syndrome (38), and inflammatory demyelinating polyradiculoneuropathy (39, 40). In our series, one patient with mixed lineage leukemia (case 8) treated with cytaribine had urinary retention, quadriparesis, and decreased deep tendon reflexes with MR enhancement of the nerve roots, although results of a meningeal biopsy revealed normal meninges. The clinical impression was inflammatory demyelinating polyradiculoneuropathy (Guillain-Barré syndrome), and the patient improved with intravenous immunoglobulin. Although patient 18 had the same MR findings of lumbosacral root enhancement, the cause proved to be leukemic relapse. Clearly, enhancement of the cauda equina in patients with leukemia warrants a vigilant search for the precipitating factor. Leptomeningeal enhancement of the brain in patients with leukemia may result from CNS relapse or infection (41, 42) or, rarely, both. Case 10 is an example of cerebral meningeal

enhancement resulting from both meningeal leukemia and bacterial meningitis (Fig 7) caused by *Acinetobacter anitratus*, which was proved with CSF cytology and CSF culture, respectively.

Before the advent of prophylactic treatment of childhood leukemia by means of CNS irradiation and intrathecal methotrexate, CNS leukemic relapse was high (2, 43). With the use of these presymptomatic therapies, survival rates increased. Unfortunately, the late effects of the prophylactic measures can result in mineralizing microangiopathy or arteriopathy, which is an injury to the small and medium-sized cerebral vasculature with calcium deposition often found in basal ganglia and subcortical white matter (6, 44, 45). Necrotizing leukoencephalopathy is characterized by a rapidly deteriorating clinical course and demyelination and necrosis of the periventricular white matter, and can be seen as early as 9 months after treatment with cranial irradiation and intrathecal methotrexate (7, 46). In our series, three patients (cases 14, 15, and 19) who had been treated with craniospinal irradiation and intrathecal methotrexate had mineralizing microangiopathy or arteriopathy and necrotizing leukoencephalopathy. Brain calcification was first noted on CT scans 3 years after initial treatment in case 15, and 4 years after treatment in cases 14 and 19. Distribution of the calcification included the subcortical white matter (case 15), bilateral basal ganglia only (case 14), and both white matter and basal ganglia (case 19), with periventricular hypodensity noted in all three patients. Mineralizing microangiopathy or arteriopathy appeared as high signal on T1-weighted images (Fig 14), a finding attributable to the surface relaxation mechanism of deposited calcium (47). Necrotizing leukoencephalopathy is typically low in signal intensity on T1-weighted images and high in signal intensity on T2-weighted images. These hyperintense T2 areas in the deep white matter also extend to more peripheral white matter.

The number of secondary malignant tumors that develop after therapy for acute lymphoblastic leukemia is 62.3 per 100 000 cases annually (48); the chance that a second tumor will develop in the CNS is even rarer (49). Although cranial irradiation (50) has clearly been implicated in the development of secondary brain tumors, cases of a second malignant tumor occurring in the CNS in survivors of childhood leukemia who had no history of prophylactic irradiation have been reported. Mechanisms such as loss of immune surveillance and genetic factors have been proposed (51). Glioma has been reported as the most common secondary brain tumor (52), followed by ependymoma, lymphoma, and meningioma. In our series, secondary brain tumors developed in three patients (cases 14, 15, and 16) 4.5 to 5.5 years after initial treatment. In two of these patients (cases 14 and 15; Figs 10 and 11, respectively), secondary gliomas developed in the setting of mineralizing microangiopathy or arteriopathy and necrotizing leukoencephalopathy. In the third patient (case 16), infected with Epstein-Barr virus after bone marrow transplantation, a primary CNS B-cell lymphoma developed 4 months after bone marrow transplantation. A second malignant tumor has been reported in connection with bone marrow transplantation (53). The occurrence of B-cell lymphoma after bone marrow transplantation or organ transplantation (54) may be the result of uncontrolled proliferation of B lymphocytes in an environment of immunosuppression. Epstein-Barr virus has been implicated in the lymphoproliferative process, which precedes malignant transformation (54, 55). These lymphomas appear hyperintense on plain CT scans and do not enhance after injection of iodinated contrast medium. The hyperdensity of the tumor masses seen on CT scans are believed to be due to hypercellularity of the tumor, a finding that was documented on microscopic examination in this case. MR imaging showed hypointense tumor signal on both T1- and T2-weighted images. The tumor did not enhance after intravenous administration of gadopentetate dimeglumine, a finding that is different from other primary or secondary CNS lymphomas, which typically enhance after contrast injection. The hypointense T2 signal of the tumors most likely also results from hypercellularity and a high nuclear/cytoplasm ratio of the tumors. These imaging characteristics might be useful in the differential diagnosis of the secondary CNS lymphoma after bone marrow transplantation for childhood leukemia.

Spinal chloroma was the initial sign of relapse in one patient (case 17) previously treated for acute myelogenous leukemia. The MR imaging findings of spinal chloroma are similar to those in the brain, in which signal is isointense with spinal cord on T1- and T2-weighted images,

and there is strong enhancement after intravenous administration of gadopentetate dimeglumine (Fig 13) (56). The epidural location of the tumor resulted in significant compression of the cervical cord. Spinal chloromas, estimated to account for 3% of all spinal tumors, are approximately as common as intracranial chloromas (57).

Summary

Neurologic complications of leukemia have increased with treatment advances and longer survival times. Improved neuroimaging techniques have helped characterize CNS abnormalities caused by direct leukemic involvement of CNS structures, cerebrovascular disorders, infections, treatment-related neurotoxicity, and second malignant tumors. Knowledge of risk factors may help in the early recognition of disease or treatment-related neurologic disorders, allowing for timely intervention.

References

1. *Cancer Facts and Figures*. Atlanta, Ga: American Cancer Society, 1987
2. Evans AE, Gilbert ES, Zandstra R. The increasing incidence of central nervous leukemia in children. *Cancer* 1970; 26:404–409
3. Niemeyer CM, Kitchcock-Bryan S, Sallan SE. Comparative analysis of treatment programs for childhood acute lymphoblastic leukemia. *Semin Oncol* 1985; 12:122–130
4. Walker RW. Neurologic complications of leukemia. *Neurol Clin* 1991; 9:989–999
5. Feinberg WM, Swenson MR. Cerebrovascular complications of L-asparaginase therapy. *Neurology* 1988; 38:127–133
6. Flament-Durand J, Ketekbant-Balasse P, Maurus R, Regnier R, Spehl M. Intracerebral calcifications appearing during the course of acute lymphocytic leukemia treated with methotrexate and X rays. *Cancer* 1975; 35:319–325
7. Rubinstein LJ, Herman MM, Long TF, Wilbur JR. Disseminated necrotizing leukoencephalopathy: a complication of treated central nervous system leukemia and lymphoma. *Cancer* 1975; 35: 291–305
8. Biti GP, Magrini SM, Vilari N, et al. Brain damage after treatment for acute lymphoblastic leukemia. *Acta Oncol* 1989; 28:253–256
9. Yim YS, Mahoney DH, Oshman DG. Hemiparesis and ischemic changes of the white matter after intrathecal therapy for children with acute lymphocytic leukemia. *Cancer* 1991; 67:2058–2061
10. Priest JR, Ramsay NKC, Steinherz PG, et al. A syndrome of thrombosis and hemorrhage complicating L-asparaginase therapy for childhood acute lymphoblastic leukemia. *Pediatrics* 1982; 100:984–989
11. Ball WS, Prenger EC, Ballard ET. Neurotoxicity of radio/chemotherapy in children: pathologic and MR correlation. *AJNR Am J Neuroradiol* 1992; 13:761–776
12. Robertson KA. Pediatric bone marrow transplantation. *Curr Opin Pediatr* 1993; 5:103–109
13. Mulhern RK, Ochs J, Fairclough D, et al. Psychoeducational status following central nervous system relapse: a retrospective analysis of 40 children treated for acute lymphoblastic leukemia. *J Clin Oncol* 1987; 5:933–940
14. Asato RA, Akiyama Y, Masatoshi I, et al. Nuclear magnetic resonance abnormalities of the cerebral white matter in children with acute lymphoblastic leukemia and malignant lymphoma during and after central nervous system prophylactic treatment with intrathecal methotrexate. *Cancer* 1992; 70:1997–2004
15. Tsuruda JS, Kortman KE, Bradley WG, Wheeler DC, Dalsem WV, Bradley TP. Radiation effects on cerebral white matter: MR evaluation. *AJNR Am J Neuroradiol* 1987; 8:431–437
16. Packer RJ, Zimmerman RA, Bilaniuk LT. Magnetic resonance imaging in the evaluation of treatment-related central nervous system damage. *Cancer* 1986; 58:635–640
17. Allen JC, Deck MDF, Howieson J, Brown M. CT scans of long-term survivors of various childhood malignancies. *Med Pediatr Oncol* 1981; 9:109–117
18. Meadows AT, Kreimas NL, Belasco JB. The medical cost of cure: sequelae in survivors of childhood cancer. In: Sullivan MP, van Eys J, eds. *Status of the Curability of Childhood Cancer*. New York, NY: Raven Press, 1980: 263–276
19. Ebner F, Ranner G, Slavc I, et al. MR findings in methotrexate-induced CNS abnormalities. *AJNR Am J Neuroradiol* 1989; 10: 959–964
20. Vaughn DJ, Jarvik JG, Hackney D, Peters S, Stadtmauer EA. High-dose cytarabine neurotoxicity: MR findings during the acute phase. *AJNR Am J Neuroradiol* 1993; 14:1014–1016
21. Valk PE, Dillon WP. Radiation injury of the brain. *AJNR Am J Neuroradiol* 1991; 12:45–62
22. Sullivan KM, Mori M, Sanders J. Late complications of allogeneic and autologous marrow transplantation. *Bone Marrow Transplant* 1992; 10(suppl 2): 127–134
23. Niemeyer CM, Hitchcock-Bryan S, Sallan SE. Comparative analysis of treatment programs for childhood acute lymphoblastic leukemia. *Semin Oncol* 1985; 12:122–130
24. Ramsay NKC, Coccia PF, Krivit W, Nesbit M, Edson JR. The effect of L-asparaginase on plasma coagulation factors in acute lymphoblastic leukemia. *Cancer* 1977; 4:1398–1401
25. Tornebohm E, Lockner D, Paul C. A retrospective analysis of bleeding complications in 438 patients with acute leukaemia during the years 1972–1991. *Eur J Haematol* 1993; 50:160–167
26. Bick RL. Coagulation abnormalities in malignancy: a review. *Semin Thromb Hemost* 1992; 18:353–371
27 Creutzig U, Ritter J, Budde M, et al. Early death due to hemorrhage and leukostasis in childhood acute myelogenous leukemia. *Cancer* 1987; 60:3071–3079
28. Collins RC, Al-Mondhiry H, Chernik NL, et al. Neurologic manifestations of intravascular coagulation in patients with cancer: a clinicopathologic analysis of 12 cases. *Neurology* 1975; 25:795–806
29. Kantarjian HM, Keating MJ, Walters RS, et al. Acute promyelocytic leukemia. *Am J Med* 1986; 80:789–797
30. Tallman MS, Kwaan HC. Reassessing the hemostatic disorder associated with acute promyelocytic leukemia. *Blood* 1992; 79: 543–553
31. Kubo M, Azuma E, Arai S, Komada Y, et al. Transient encephalopathy following a single exposure of high-dose methotrexate in a child with acute lymphoblastic leukemia. *Pediatr Hematol Oncol* 1992; 9:157–165
32. Bodey GP. Infection in cancer patients: a continuing association. *Am J Med* 1986; 81(suppl 1A):11–26
33. Salonen J, Nikoskelainen J. Lethal infections in patients with hematological malignancies. *Eur J Haematol* 1993;51:102–108

34. Anderson D, Matick H, Naheedy MH, Stein K. Rhinocerebral mucormycosis with CT scan findings: a case report. *Comput Radiol* 1984; 8:113–117
35. Gamba JL, Woodruff WW, Djang WT, Yeates AE. Craniofacial mucormycosis: assessment with CT. *Radiology* 1986; 160:207–212
36. Fellows DW, King VD, Conturo T, et al. In vitro evaluation of MR hypointensity in aspergillus colonies. *AJNR Am J Neuroradiol* 1994 15:1139–1141
37. Sze G. Gadolinium-DTPA in spinal disease. *Radiol Clin North Am* 1988; 26:1009–1024
38. Bazan C III, Jackson C, Jinkins JR, Barohn RJ. Gadolinium-enhanced MRI in a case of cytomegalovirus polyradiculopathy. *Neurology* 1991; 41:1522–1523
39. Morgan GW, Barohn RJ, Bazan C III, King RB, Klucznick RP. Nerve root enhancement with MRI in inflammatory demyelinating polyradiculoneuropathy. *Neurology* 1993; 43:618–620
40. Georgy BA, Chong B, Chamberlain M, Hesselink JR, Cheung G. MR of the spine in Guillain-Barré syndrome. *AJNR Am J Neuroradiol* 1994; 15:300–301
41. David PC, Friedman NC, Fry SM, et al. Leptomeningeal metastasis: MR imaging. *Radiology* 1987; 163:449–454.
42. Mathews VP, Kuharik MA, Edwards MK, et al. Gd-DTPA enhanced MR imaging of experimental bacterial meningitis: evaluation and comparison with CT. *AJNR Am J Neuroradiol* 1988; 9:1045–1050
43. Pinkel D. Patterns of failure in acute lymphocytic leukemia. *Cancer Treat Sympt* 1983; 2:259–266
44. Price RA, Birdwell DA. The central nervous system in childhood leukemia, III: mineralizing microangiopathy and dystrophic calcification. *Cancer* 1978; 42:717–728
45. Biti GP, Magrini SM, Villari N, et al. Brain damage after treatment for acute lymphoblastic leukemia: a report on 34 patients with special regard for MRI findings. *Acta Oncol* 1989; 28:253–256
46. Price RA, Jamieson PA. The central nervous system in childhood leukemia, II: subacute leukoencephalopathy. *Cancer* 1975; 35: 306–318
47. Henkelman RM, Watts JF, Kucharczyk W. High signal intensity in MR imaging of calcified brain tissue. *Radiology* 1991; 179:199–206
48. Mike V, Meadows AT, D'Angio GD. Incidence of second malignant neoplasms in children: results of an international study. *Lancet* 1982; 2:1326–1331
49. Malone M, Lumley H, Erodohazi M. Astrocytoma as a second malignancy in patients with acute lymphoblastic leukemia. *Cancer* 1986; 57:1979–1985
50. Modan B, Mar H, Braidtz D, et al. Radiation-induced head and neck tumors. *Lancet* 1974; 1:277–279
51. Gilman PA, Miller RW. Cancer after acute lymphoblastic leukemia. *Am J Dis Child* 1981; 135:311–312
52. Zarrabi MH, Rosner F, Grunwald HW. Second neoplasms in acute lymphoblastic leukemia. *Cancer* 1983; 52:1712–1719
53. Witherspoon RP, Fisher LD, Schoch G, et al. Secondary cancers after bone marrow transplantation for leukemia or aplastic anemia. *N Engl J Med* 1989; 784–789
54. Zutter MM, Martin PJ, Sale GE, et al. Epstein-Barré virus lymphoproliferation after bone marrow transplantation. *Blood* 1988; 72: 520–529
55. Patton DF, Wilkowski CW, Hanson CA. Epstein-Barr virus determined clonality in posttransplant lymphoproliferative disease. *Transplantation* 1990; 49:1080–1084
56. Leonard KJ. MR appearance of intracranial chloromas. *AJNR Am J Neuroradiol* 1989; 10(suppl):67–68
57. Petursson SR, Boggs DR. Spinal cord involvement in leukemia: a review of the literature and a case of Ph' + acute myeloid leukemia presenting with a conus medullaris syndrome. *Cancer* 1981; 47:346–350